



FAST ESTIMATION OF WOOD ELASTIC CONSTANTS USING LEAST-SQUARES

Sebastian Duran^{1*}

Michele Ducceschi¹

Henna Tahvanainen¹

Ludovico Ausiello²

¹ Department of Industrial Engineering, University of Bologna, Italy

² SENE, University of Portsmouth, Portsmouth, Hampshire, UK

ABSTRACT

Mechanical properties of materials represent, among others, one of the most relevant topics in musical acoustics. Such features can be used to better understand the behaviour of musical instruments or to evaluate the impact of design interventions, and build accurate physical models. In this regard, this paper aims to introduce an accessible procedure to estimate the elastic constants of wood using a thin plate. Compared to previous methods in the literature, the inverse problem is here formulated linearly in the rigidity constants, thus allowing a unique solution via a matrix inverse, and using a least-squares formulation. The reliability of the method is numerically proven in a number of examples.

Keywords: *experimental modal analysis, finite element method, elastic constants, wood*

1. INTRODUCTION

The problem of determining the elastic constants of wood emerges in various applications in sound synthesis and luthiery. Possible applications vary from the virtual prototyping of musical instruments, allowing for faster and more efficient product development processes [1], to model-aided conservation of historical instruments [2] and to sound synthesis purposes requiring accurate input

data to generate realistic models [3]. Often, the elastic constants of woods are approximated from literature [4,5]. Nonetheless, the impact of the material and its elastic constants proved to be both mechanically quantifiable as well as perceptually noticeable [6, 7]. When an accurate estimation of such properties is needed, two main approaches are defined, namely destructive or non-destructive methods [8]. While the first represents an invasive analysis method based on static loading tests, non-destructive methods take advantage of experimental and numerical approaches. Numerical non-destructive approaches are further distinguished between forward and inverse approaches. In the first case, the Finite Element Method (FEM) is prevalent [8] although recent research advancements focused on the potential of the Rayleigh method to estimate elastic constants for different boundary conditions [9]. On the other hand, inverse processes mainly involve the minimization of an objective function which is normally defined in terms of the difference between experimental and computed eigenfrequencies [10, 11]. In this regard, a recent example presented in [12] consisted of measuring the eigenfrequencies of the plate and using the theory of free orthotropic plates to determine the elastic constants. Previously, the measurement of three out of four independent elastic constants was proposed for plates with free edges [13]. Possibilistic identification has also been applied in conjunction with FEM to obtain a range of possible parameter values of a complete instrument [14]. The existing methods for material identification involve specific boundary conditions, and the determination of several eigenfrequencies by computation, measurement or both. The aim of the presented study is to introduce an alternative and accessible methodology allowing retrieval of

*Corresponding author: sebastian.duran2@unibo.it.

Copyright: ©2023 Sebastian Duran et. al This is an open-access article distributed under the terms of the Creative Commons Attribution 3.0 Unported License, which permits unrestricted use, distribution, and reproduction in any medium, provided the original author and source are credited.



the rigidity constants of orthotropic materials by adopting a simple experimental measurement setup and by taking advantage of the least-square problem optimization. As opposed to other methods in the literature, such as [10], the problem is here formulated linearly in the rigidity constants, allowing for their direct estimation via a matrix inversion. Furthermore, the method can be applied to plates subjected to any combination of boundary conditions, thus facilitating the experimental setup. Here, a benchmark study is numerically conducted to validate the experimental methodology. Error and convergence analyses are performed, showing the ability of the proposed method to retrieve the correct rigidity constants within reference error bounds.

2. METHODOLOGY

An accurate estimation of wood elastic constant is a difficult task. Complications arise in some cases due to the complex geometry of the specimen under study, such as for violin plates [11], or due to a complex material structure, such as for composite plates [10]. However, if a thin, homogeneous rectangular plate of the specimen is available, it is possible to extract the thin-plate rigidity constants with relative ease. This work presents one such methodology, aimed at integrating various other methods found in literature [9, 13]. The core principle of the proposed method lies in the semi-analytical form of the orthotropic thin-plate eigenfrequencies. In measurement or simulation, these are usually sorted in ascending order, via the integer $m \in \mathbb{N} = \{1, 2, \dots\}$. The m^{th} eigenfrequency is thus [12]:

$$\omega^m = \sqrt{\frac{\pi^4}{\rho L_x^4} (D_x \alpha_x^m + \sigma^4 D_y \alpha_y^m + \sigma^2 D_{xy} \alpha_{xy}^m)}. \quad (1)$$

Above, the three rigidity constants (to be estimated) are denoted by D_x, D_y, D_{xy} . These are defined as:

$$D_x = \frac{E_x h^3}{12(1 - \nu_{xy} \nu_{yx})}, \quad (2a)$$

$$D_y = \frac{E_y h^3}{12(1 - \nu_{xy} \nu_{yx})}, \quad (2b)$$

$$D_{xy} = \nu_{yx} D_x + \nu_{xy} D_y + \frac{G_{xy} h^3}{3}, \quad (2c)$$

where E_x, E_y are the Young's moduli, ν_{xy}, ν_{yx} are the Poisson's ratios, G_{xy} is the shear modulus, and h is the thickness, assumed uniform across the domain. Furthermore, in (1), ρ denotes the surface density, L_x is the side

length in the longitudinal x direction (assumed here to be along the grain), $\sigma := L_x/L_y$ is the aspect ratio, and L_y is the side length in the radial y direction (across the grain). Leaving aside the geometric constants and the density, which may be measured trivially, the rigidity constants depend on five unknown parameters (two Young's moduli, the shear modulus and two Poisson's ratios). These may be reduced to four via symmetry of the compliance matrix, giving e.g. $\nu_{yx} = \nu_{xy} E_y / E_x$ [15]. The proposed method allows measuring three such constants, via (2). Given the small variation of Poisson's ratios across specimens [5], one may fix ν_{xy} according to tabulated values, and therefore extract E_x, E_y and G_{xy} . Alternatively, an independent measurement of any one of the four unknown elastic constants allows fixing the other three (one such measurement will be briefly discussed later, in Section 3.3).

For rectangular geometries, it is customary to associate a pair of modal numbers $(\mu_x^m, \mu_y^m) \in \mathbb{N}^2$ to each mode, related to the number of nodal lines in the x and y directions. A key feature of (1) is that the α coefficients depend exclusively on the boundary conditions and on the modal numbers. This results immediately from a dimensional analysis of (1), where such coefficients have the interpretation of scaled (i.e. non-dimensional) wavenumbers. One may express such dependency as:

$$\alpha_x^m := \alpha_x(\mu_x^m, \mu_y^m | \mathcal{B}), \quad (3)$$

where \mathcal{B} denotes a set of boundary conditions. Similar definitions hold for $\alpha_y^m, \alpha_{xy}^m$. As an example, under simply-supported boundary conditions, a time-harmonic solution to the orthotropic plate equation is obtained as [16]:

$$u(x, y, t) = \hat{u} \sin \frac{\mu_x^m \pi x}{L_x} \sin \frac{\mu_y^m \pi y}{L_y} e^{j\omega t}, \quad (4)$$

and hence:

$$\alpha_x^m = (\mu_x^m)^4, \quad \alpha_y^m = (\mu_y^m)^4, \quad \alpha_{xy}^m = 2(\mu_x^m)^2(\mu_y^m)^2.$$

The α coefficients for other boundary conditions are not readily available, though they may be computed numerically, as will be illustrated in Section 2.2.

2.1 Problem Formulation

Let $\mathfrak{P} := \{L_x, L_y, \rho, h, D_x, D_y, D_{xy} | \mathcal{B}\}$ denote a set of geometrical and material parameters of an experimental plate. All the parameters are assumed known except for the rigidity constants. The experimental plate is subjected

to a set of boundary conditions \mathcal{B} , for which the α coefficients are known either analytically or numerically. After squaring both sides and rearranging terms, one may express a vector version of (1) as:

$$\mathbf{p} = \mathbf{A}\mathbf{d}, \quad (5)$$

where

$$(\mathbf{p})^m := \rho(\omega^m)^2/\pi^4, \quad (6a)$$

$$(\mathbf{A})^{m,:} := [\alpha_x^m, \sigma^4 \alpha_y^m, \sigma^2 \alpha_{xy}^m]/L_x^4, \quad (6b)$$

$$\mathbf{d} := [D_x, D_y, D_{xy}]^\top. \quad (6c)$$

Here, $m \in [1, M]$, and thus \mathbf{p} is $M \times 1$, and \mathbf{A} is $M \times 3$. Assume as well that a set of modal frequencies $\hat{\omega}^m$, is obtained experimentally, so to yield a vector $(\hat{\mathbf{p}})^m := \rho(\hat{\omega}^m)^2/\pi^4$. Then, the vector $\hat{\mathbf{d}}$ of unknown rigidity constants, approximating \mathbf{d} in (5), can be obtained by minimising:

$$\varepsilon(\hat{\mathbf{d}}|\hat{\mathbf{p}}) := \frac{1}{2} \|\mathbf{A}\hat{\mathbf{d}} - \hat{\mathbf{p}}\|_2^2, \quad (7)$$

where $\|\circ\|_2$ denotes the Euclidian norm. This is a linear-in-parameters equation, solved by the least-squares formula. Thus:

$$\hat{\mathbf{d}} = (\mathbf{A}^\top \mathbf{A})^{-1} (\mathbf{A}^\top \hat{\mathbf{p}}). \quad (8)$$

This is, in essence, the core of the presented method. While simple, it will be shown to yield accurate results.

2.2 Numerical calculation of the α coefficients

As mentioned previously, the α coefficients are generally not known. These, however, can be computed numerically using a least-square approximation. To that end, assume to work with a number N_{train} of “training” plates, with plate parameters $\mathfrak{P}^n := \{L_x^n, L_y^n, \rho, h, D_x, D_y, D_{xy} | \mathcal{B}\}$, $n \in [1, N_{train}]$. Note that the sets \mathfrak{P}^n differ only in the side lengths L_x^n, L_y^n and associated aspect ratios σ^n , but share the same values of all the other parameters, and have the same boundary conditions. Then, for plate n , one may label the frequencies according to the corresponding modal numbers (μ_x, μ_y) , that is: $\omega_{(1,1)}^n, \omega_{(1,2)}^n, \dots, \omega_{(\mu_x, \mu_y)}^n$. For a given pair on indices (μ_x, μ_y) , one may then write a vector version of (1) as:

$$\mathbf{q} = \mathbf{D}\mathbf{a}, \quad (9)$$

where

$$(\mathbf{q})^n := \rho(\omega_{(\mu_x, \mu_y)}^n)^2/\pi^4, \quad (10a)$$

$$(\mathbf{D})^{n,:} := [D_x, (\sigma^n)^4 D_y, (\sigma^n)^2 D_{xy}]/(L_x^n)^4, \quad (10b)$$

$$\mathbf{a} := [\alpha_x(\mu_x, \mu_y), \alpha_y(\mu_x, \mu_y), \alpha_{xy}(\mu_x, \mu_y)]^\top. \quad (10c)$$

Here, $n \in [1, N]$, and thus \mathbf{q} is $N \times 1$, and \mathbf{D} is $N \times 3$. Assume now to extract a vector $(\hat{\mathbf{q}})^n := \rho(\hat{\omega}_{(\mu_x, \mu_y)}^n)^2/\pi^4$ from e.g. finite-element simulation of the N_{test} plates with parameters \mathfrak{P}^n . Then, one minimises the error:

$$\varepsilon(\hat{\mathbf{a}}|\hat{\mathbf{q}}) := \frac{1}{2} \|\mathbf{D}\hat{\mathbf{a}} - \hat{\mathbf{q}}\|_2^2, \quad (11)$$

which is solved by:

$$\hat{\mathbf{a}} = (\mathbf{D}^\top \mathbf{D})^{-1} (\mathbf{D}^\top \hat{\mathbf{q}}). \quad (12)$$

This vector returns an approximation to \mathbf{a} in (9). This operation can be repeated to compute the α coefficients needed to build the matrix \mathbf{A} in (6b), according to the specified boundary conditions of the experimental plate.

3. NUMERICAL EXAMPLES

The methodology described in Section 2 is tested in a number of validation experiments. The experiments are here conducted numerically, so to assess the ability of the proposed method to retrieve the correct elastic constants. This is a necessary step before moving on to the experimental case. Two “experimental” plates with a known set of parameters are created numerically, and the eigenfrequencies of each plate are used to estimate the rigidity constants via (8). These are then compared with the input constants. The “experimental” plate parameters are summarised in Table 1.

Type	ρ (kg/m ³)	E_x (MPa)	E_y (MPa)	G_{xy} (MPa)	ν_{xy}	σ
Fir	0.225	$127 \cdot 10^2$	$9.3 \cdot 10^2$	$9.3 \cdot 10^2$	0.45	1.5
Balsa	0.100	$6.3 \cdot 10^2$	$3 \cdot 10^2$	$3.1 \cdot 10^2$	0.23	0.8

Table 1. Constants for the “experimental” plates, wood properties obtained from [5]. σ denotes the aspect ratios for plates 1 and 2, respectively. The plate thickness is $h = 0.5$ mm.

Two different sets of boundary conditions are considered: simply supported and clamped. For the simply supported boundary condition, an analytical solution for the α coefficients exists in the form (4). For the clamped boundary condition, the α coefficients have to be computed numerically. The workflow of the proposed methodology is summarised as follows:

1. For the experimental plate under study, recover a set of M α coefficients. Such coefficients, depend-

ing exclusively on the boundary conditions imposed on the experimental plate and on the modal numbers, may be available analytically, or they may be computed numerically via (12).

2. Perform a modal analysis of the experimental plate to measure the M eigenmodes corresponding to the α coefficients above and use (8) to compute the rigidity constants.

Note that step 1. above may be entirely avoided if tables of α coefficients, under various combinations of boundary conditions, are made available to the tester. The authors intend to provide such tables in the future. It is also anticipated that the measurement of $M = 3$ eigenmodes suffices for an accurate estimation of the three rigidity constants.

3.1 Simply Supported boundary conditions

In the following, a plate with simply supported edges is considered. While the α coefficients are also known analytically in this case, via (4), they will nonetheless be computed using (12) with a set of plates, and the result fed into (8) to extract the rigidity constants. This serves as a useful benchmark test for the current methodology.

Type	ρ (kg/m ²)	E_x (MPa)	E_y (MPa)	G_{xy} (MPa)	ν_{xy}
Sitka sp.	0.195	$116 \cdot 10^2$	$9 \cdot 10^2$	$7.5 \cdot 10^2$	0.37

Table 2. Thin-plate elastic constants for the “training” plates in $TS1$ used to calculate the α coefficients in the simply-supported case. Values are typical of Sitka spruce (*Picea sitchensis*) obtained from [5]. The plate thickness is $h = 0.5$ mm.

A number $N_{train} = 16$ of plates is used to define training set 1 ($TS1$). The side lengths L_x, L_y of such plates are obtained as all the possible combinations of the set $\{0.1, 0.53, 0.97, 1.4\}$ m. The other elastic and geometric constants for $TS1$ are reported in Table 2. Using such material and geometrical parameters, the eigenfrequencies of all 16 plates are computed analytically via (4). Then, the corresponding α values are computed via (12), for $(\mu_x, \mu_y) \in [0, 9]$. Successively, the modal frequencies of the two “experimental” plates from Table 1 are computed, using the closed-form solution (4). The least-square procedure (8) is run to retrieve the elastic constants. These can be now compared to the input elastic constants

of the “experimental” plates reported in Table 1. An absolute error of the order of 10^{-11} for both plates is recovered between the computed and input elastic constants.

3.2 Clamped boundary conditions

In a second test case, a plate with fully clamped edges is considered. Contrary to the simply-supported case, neither the eigenfrequencies nor the α coefficients are available in closed form. Hence, they can only be recovered numerically. The same set of test plates $TS1$ defined in Section 3.1 is initially used. To check the assumption that the α coefficients only depend on the modal numbers, but not on the geometrical or material properties, two more training sets are defined here ($TS2$ and $TS3$). These present different side lengths $L_x = L_y = \{0.5, 0.77, 1.03, 1.3\}$ m and $L_x = L_y = \{0.5, 0.8, 1.1, 1.4\}$ m for $TS2$ and $TS3$, respectively, as well as different material parameters, summarised in Table 3. COMSOL 6.0 is used for the calculation of the

TS1 and TS3

ρ (kg/m ²)	E_x (MPa)	E_y (MPa)	G_{xy} (MPa)	ν_{xy}
0.195	$116 \cdot 10^2$	$9 \cdot 10^2$	$7.5 \cdot 10^2$	0.37
E_z (MPa)	G_{yz} (MPa)	G_{xz} (MPa)	ν_{yz}	ν_{xz}
$5 \cdot 10^2$	$0.39 \cdot 10^2$	$7.2 \cdot 10^2$	0.43	0.47

TS2

ρ (kg/m ²)	E_x (MPa)	E_y (MPa)	G_{xy} (MPa)	ν_{xy}
0.225	$127 \cdot 10^2$	$9.3 \cdot 10^2$	$9.3 \cdot 10^2$	0.45
E_z (MPa)	G_{yz} (MPa)	G_{xz} (MPa)	ν_{yz}	ν_{xz}
$4.8 \cdot 10^2$	$9.3 \cdot 10^2$	$7.5 \cdot 10^2$	0.60	0.50

Table 3. Thin and thick plate elastic constants for the “training” plates (used in the calculation of the α coefficients of a fully clamped plate). The plates’ thickness is $h = 0.5$ mm for all plates.

eigenfrequencies of the training plates from each of the three TS s. Note that Table 3 reports the thick-plate constants as well as the thin-plate ones, as COMSOL requires the specification of all these. However, since the plate are simulated with a very small thickness ($h = 0.5$ mm), it can be assumed that the thick-plate constants will have a negligible influence on the computation of the α coeffi-

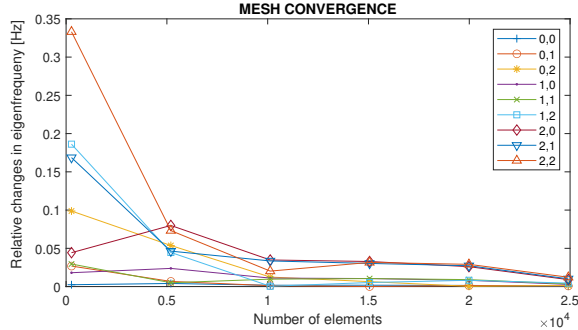


Figure 1. Relative differences in eigenfrequency for a fully clamped orthotropic plate. Predefined-only meshes ranging from *coarser* to *extremely fine* were used in COMSOL to conduct this study.

cients. The point of selecting such a small h is to minimise the thick-plate effects during benchmarking. The predefined *extremely fine* mesh in COMSOL was used at this stage to guarantee reliable results. A quick check on the convergence of the eigenfrequencies was conducted with respect to mesh refinement for the first modes with indices $(\mu_x, \mu_y) \in [0, 2]$. To this end, a plate from *TS1* with an aspect ratio $\sigma = 1$ is taken into account. As an illustrative example, Figure 1 reports the convergence study on a square plate with side lengths of 1.4 m x 1.4 m. As reported in Figure 1, by employing the highest number of elements given by the *extremely fine* mesh, the relative change in eigenfrequencies is reached up to 0.001 Hz (i.e. eigenfrequencies converge up to two decimal places) for the lowest-order modes. On the other hand, the change at higher-order modes increases up to 0.01 Hz (i.e. eigenfrequencies converge up to one decimal place). Thus, a maximum error equal to 0.01 Hz is assumed in the eigenfrequency calculation.

The calculation of the α coefficients is now performed as per (12), using all three training sets. The results are displayed in Figure 2 where the average values for such coefficients are reported, together with the deviation. The deviation is seen to increase for higher modal numbers, as the error in the calculation of the corresponding modal frequencies is higher. The α coefficients from the three training sets and from an additional set obtained by averaging are now used to obtain various estimates of the rigidity constants, via (8). It is interesting to check how the error on the computed constants changes according to the size of \mathbf{A} in (8). This is done in Figure 3, where subsets

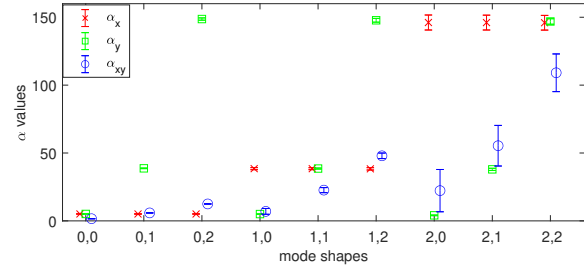


Figure 2. Average α coefficients and deviations, under fully clamped boundary conditions. 'x' marker: α_x , '□' marker: α_y , 'o' marker: α_{xy} .

of the available α coefficients, denoted $G_{\alpha n}$, $n=\{1, 2, 3\}$, are used for the calculation of the rigidity constants. Here, $G_{\alpha n}$ contains the first $3n$ coefficients, out of the nine available. It can be seen that for all the evaluated groups of constants $G_{\alpha n}$, errors are the smallest for $G_{\alpha 1}$. Furthermore, the error depends on the test plate, and on the training set used to compute the α coefficients. In particular, the largest errors are found when computing the α coefficients by using *TS1*. Instead, for *TS2* and *TS3*, the errors are of a similar order. The dependence of the error on the size of \mathbf{A} is to be attributed to the error on the estimation of the eigenfrequencies themselves, and to the propagation of such error via the least-square procedure. Further investigation is underway in this sense. Results from $G_{\alpha 1}$ are summarised in Table 4, highlighting the accuracy achievable with the proposed methodology.

3.3 Independent measurement of E_x

With the proposed methodology, it is possible to obtain three out of the four thin plate elastic constants. An independent measurement of any one of the elastic constants is thus necessary to estimate all four uniquely. One such experiment is briefly described here. Consider a bar with free edges, where the x axis is stretched along the bar. It is known that the m^{th} longitudinal modal frequency satisfies:

$$\omega^m = \sqrt{E_x/\varrho} \gamma^m, \quad (13)$$

where ϱ is the volume density, and $\gamma^m := m\pi/L_x$. Figure 4 reports the frequency response of a metal bar, hit with an impulse hammer at one end and measured with an accelerometer placed at the opposite end. The peaks corresponding to the longitudinal bar motion are clearly visible, and a best fit of model (13) allows to extract the

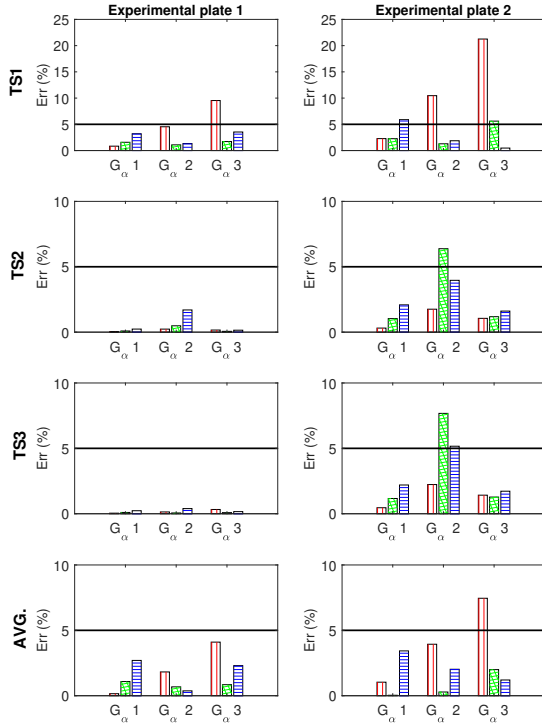


Figure 3. Error% for rigidity constants D_x (vertical lines), D_y (crossing lines) and D_{xy} (horizontal lines) obtained by employing the α values from each TS and the α coefficients averaged over the three TS s, under fully clamped boundary conditions. Rigidity constant results for $G_{\alpha}1$, $G_{\alpha}2$ and $G_{\alpha}3$ are estimated by using the “experimental” eigenfrequencies and the related modal shapes with indices (μ_x, μ_y) up to (0,2), (1,2) and (2,2), respectively.

longitudinal speed of sound, $\sqrt{E_x/\rho}$, and, thus, Young’s modulus. The same experiment may be repeated on a bar cut from the same wood specimen of the orthotropic plate under study.

4. DISCUSSION

The numerical examples in Section 3 demonstrate the feasibility of the proposed methodology for obtaining the rigidity constants under different boundary conditions. The results shown suggest that only three modes of the investigated experimental plate are required to achieve a fairly accurate estimate of the material’s rigidity con-

<i>Experimental plate 1</i>					
Rigidity ($\times 10^{-3}$)	Target	$TS1$	$TS2$	$TS3$	AVG.
D_x	134	133	134	134	134
D_y	9.83	9.99	9.82	9.82	9.88
D_{xy}	47.6	46.1	47.7	47.5	47.1
<i>Experimental plate 2</i>					
Rigidity ($\times 10^{-3}$)	Target	$TS1$	$TS2$	$TS3$	AVG.
D_x	6.73	6.58	6.71	6.70	6.66
D_y	3.21	3.28	3.17	3.17	3.21
D_{xy}	14.4	13.5	14.1	14.1	13.9

Table 4. Results of the proposed methodology. The table includes the target and the computed rigidity constants for the two “experimental” plates considered, under clamped boundary conditions, using group $G_{\alpha}1$. Values are scaled by 10^{-3} .

stants. This means that the estimation of the constants can be done with a simple measurement setup giving the first three mode frequencies, their corresponding nodal lines and a least-square procedure. As opposed to other established methods in the literature, the proposed methodology is not bound to a restricted set of boundary conditions, nor is it reliant on specific mode shapes to work. The rigidity constants here can be estimated by knowledge of any three modal frequencies and corresponding α coefficients. Nonetheless, several sources of uncertainty regarding the methodology need to be further analysed. First, the choice of the dimensions of the plates used for the estimation of the α coefficients appeared to have an impact on the accuracy of the final estimated elastic constants. Specifically, results achieved by considering $TS1$ which was characterized by narrower rectangular-shaped geometries than $TS2$ and $TS3$, lead to a less accurate final estimation of the elastic properties of the “experimental” plates. Similarly, as α coefficients associated with higher-order mode shapes are divergent, a thorough analysis of the convergence of the coefficients is needed. These issues may be tackled by analysing the error propagation in the least-square optimisation, and by using variants of such methodology [17]. Additionally, further investigations supported by FEM simulations will be conducted in order to assess the variation in the alpha coefficient relative to changes in thickness. Such a tolerance analysis

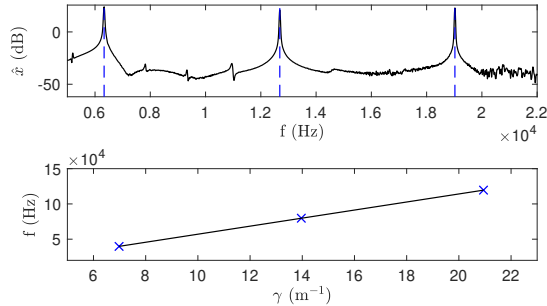


Figure 4. Modal analysis of a longitudinal bar. The bar's length L_x is 0.45 m. Top: frequency response function. Bottom: best fit. The speed of sound is here calculated as $\sqrt{E_x/\rho} = 5704 \text{ m}\cdot\text{s}^{-1}$.

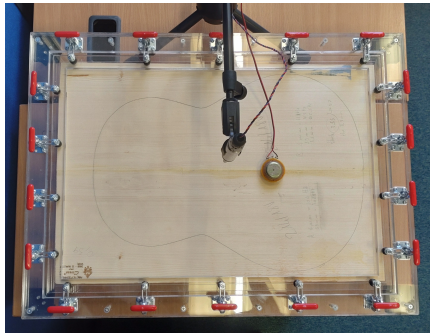


Figure 5. EMA measurement setup for a rectangular guitar tonewood under fully-clamped conditions.

will help to account for typical standard deviations observed when using standard mechanical equipment (e.g. sanding devices). Although this paper solely considers numerical data, experimental modal analysis (EMA) measurements are currently being conducted by the authors in order to test the proposed methodology with real-life case scenarios. An example is found in Figure 5 which shows a measurement setup used to extract the experimental data through impulse response (IR) measurements. In this case, an exciter is used to excite a clamped rectangular tonewood for a guitar plate by injecting an exponential sine sweep (ESS) into the system. The resulting audio data is recorded by a sound-pressure microphone. After post-processing the recorded data, an IR can be collected and analyzed [18, 19]. In such measurements, the effect of the thickness of actual instruments' soundboards (≈ 3 -

4 mm) on the methodology will also be studied. Finally, note that while simply-supported and clamped boundary conditions were considered here, one may apply the proposed method to any set \mathcal{B} of suitable boundary conditions, after an appropriate estimation of the α coefficients. These may in fact be collected and tabulated and made readily available to the tester.

5. CONCLUSIONS

This paper introduced an alternative solution to estimate orthotropic elastic constants of simple rectangular geometries under different boundary conditions through a least-square optimisation. The developed procedure was first tested for simply-supported plates for which an analytical solution to the motion equation is known. Results confirm the accuracy of the process and further investigations are carried out to compute the elastic constants of rectangular wooden plates with clamped boundary conditions. In such cases, different considerations are observed:

- Depending on the geometries used in the TS s to compute the α coefficients, different errors were observed in the estimation of the elastic constants.
- variations in the α coefficients increased with higher-order modal shapes, leading to a less precise estimation of α values.
- accurate estimates of the rigidity constants (with absolute errors below 5%) can be achieved with just three known modal shapes and the corresponding eigenfrequencies of the experimental plate.

The variability in the estimation of the rigidity constants has to be attributed to the propagation of the error in the least-square procedure. This may be adjusted in various ways, for instance via regularisation [17]. A study of optimal conditions for optimisation is therefore envisaged. Finally, the application of this methodology to laboratory tests is currently underway. Since this method allows the extraction of the rigidity constants under any combination of boundary conditions, multiple estimates may be performed on the same test bench, improving the reliability of the final results.

6. ACKNOWLEDGMENTS

This work was supported by the European Research Council (ERC), under grant 2020-StG-950084-NEMUS. HT's work has been supported by the Finnish Cultural Foundation.

7. REFERENCES

- [1] H. Tahvanainen, H. Matsuda, and R. Shinoda, “Numerical simulation of the acoustic guitar for virtual prototyping,” *Proc. of ISMA 2019*, pp. 13–17, 2019.
- [2] R. Viala, V. Placet, S. Le Conte, S. Vaiedelich, and S. Cogan, “Model-based decision support methods applied to the conservation of musical instruments: Application to an antique cello,” in *Model Validation and Uncertainty Quantification, Volume 3: Proc. of the 37th IMAC, A Conference and Exposition on Structural Dynamics 2019*, pp. 223–227, Springer, 2020.
- [3] S. Bilbao, *Numerical sound synthesis: finite difference schemes and simulation in musical acoustics*. John Wiley & Sons, 2009.
- [4] D. E. Kretschmann, “Mechanical properties of wood,” *Environments*, vol. 5, p. 34, 2010.
- [5] V. Bucur, *Acoustics of wood*. Springer Science & Business Media, 2006.
- [6] R. Viala, M. A. Pérez, V. Placet, A. Manjon, E. Foltête, and S. Cogan, “Towards model-based approaches for musical instruments making: validation of the model of a spanish guitar soundboard and characterization features proposal,” *Applied Acoustics*, vol. 172, p. 107591, 2021.
- [7] S. Merchel, M. E. Altinsoy, and D. Olson, “Perceptual evaluation of bracewood and soundboard wood variations on the preference of a steel-string acoustic guitar,” *The Journal of the Acoustical Society of America*, vol. 146, no. 4, pp. 2608–2618, 2019.
- [8] J. H. Tam, Z. C. Ong, Z. Ismail, B. C. Ang, and S. Y. Khoo, “Identification of material properties of composite materials using nondestructive vibrational evaluation approaches: A review,” *Mechanics of Advanced Materials and Structures*, vol. 24, no. 12, pp. 971–986, 2017.
- [9] J. Zhou, Y. H. Chui, M. Gong, and L. Hu, “Comparative study on measurement of elastic constants of wood-based panels using modal testing: choice of boundary conditions and calculation methods,” *Journal of Wood Science*, vol. 63, no. 5, pp. 523–538, 2017.
- [10] S.-F. Hwang, J.-C. Wu, and R.-S. He, “Identification of effective elastic constants of composite plates based on a hybrid genetic algorithm,” *Composite Structures*, vol. 90, no. 2, pp. 217–224, 2009.
- [11] R. Viala, V. Placet, and S. Cogan, “Identification of the anisotropic elastic and damping properties of complex shape composite parts using an inverse method based on finite element model updating and 3d velocity fields measurements (femu-3dvf): Application to bio-based composite violin soundboards,” *Composites Part A: Applied Science and Manufacturing*, vol. 106, pp. 91–103, 2018.
- [12] C. Guan, H. Zhang, X. Wang, H. Miao, L. Zhou, and F. Liu, “Experimental and theoretical modal analysis of full-sized wood composite panels supported on four nodes,” *Materials*, vol. 10, no. 6, p. 683, 2017.
- [13] M. McIntyre and J. Woodhouse, “On measuring the elastic and damping constants of orthotropic sheet materials,” *Acta Metallurgica*, vol. 36, no. 6, pp. 1397–1416, 1988.
- [14] A. Brauchler, D. Hose, P. Ziegler, M. Hanss, and P. Eberhard, “Distinguishing geometrically identical instruments: Possibilistic identification of material parameters in a parametrically model order reduced finite element model of a classical guitar,” *Journal of Sound and Vibration*, vol. 535, p. 117071, 2022.
- [15] A. Wilczyński and M. Kociszewski, “Determination of elastic constants of particleboard layers by compressing glued layer specimens,” *Wood Research*, vol. 56, no. 1, pp. 77–91, 2011.
- [16] A. W. Leissa, *Vibration of plates*, vol. 160. Washington, DC, USA: Scientific and Technical Information Division, National Aeronautics and Space Administration, 1969.
- [17] C. R. Rao, H. Toutenburg, Shalabh, and C. Heumann, *Linear Models and Generalizations: Least Squares and Alternatives*. Springer Publishing Company, Incorporated, 3rd ed., 2007.
- [18] L. Ausiello, L. Yule, G. Squicciarini, and C. Barlow, “Guitar soundboard measurements for repeatable acoustic performance manufacturing,” in *Proc. Reproduced Sound 2018*, (Bristol, UK), 27–29 November 2018.
- [19] L. Ausiello and V. Hockey, “Quantitative measurements to enhance performance of acoustic musical instruments and improve manufacturing,” *Acoustic Bulletin*, vol. 47, no. 2, 2021.